CrystEngComm

Accepted Manuscript

ROYAL SOCIETY OF CHEMISTRY

www.rsc.org/crystengcomm

Synthesis of a Series of Coordination Polymers Based on Mixed Ligands to Tune the Structural Dimension

Xinyu Cao, Bao Mu, Rudan Huang*

Key Laboratory of Cluster Science of Ministry of Education, School of Chemistry, Beijing Institute of Technology, Beijing 100081, PR China E-mail: huangrudan1@bit.edu.cn

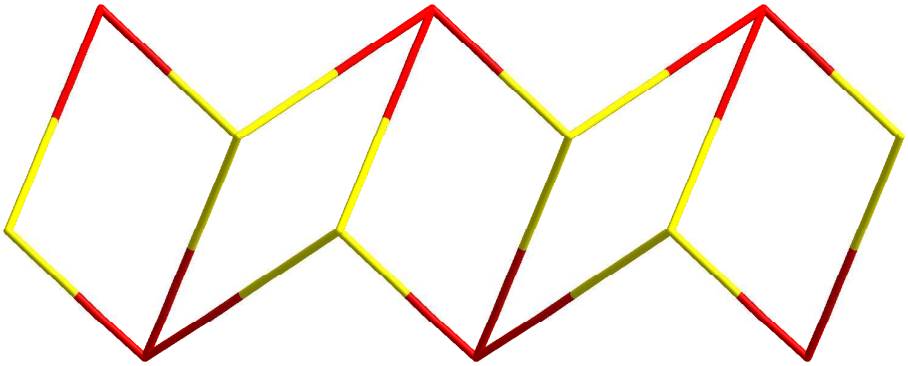

Schematic illustrating the 2D network of complex **1**. Color code: yellow, Mn, cob^{2-} ligand: red.

*Corresponding author. tel./fax: 0086-010-68912667 (R. D. Huang);
Email: huangrd@bit.edu.cn (R. D. Huang).

Cite this: DOI: 10.1039/c0xx00000x

www.rsc.org/xxxxxx

ARTICLE TYPE

Synthesis of a Series of Coordination Polymers Based on Mixed Ligands to Tune the Structural Dimension

Xinyu Cao, Bao Mu, Rudan Huang*

Eight coordination polymers, namely, Mn(cob)(phen) (**1**), Co(cob)(phen)$_2$(H$_2$O)·5H$_2$O (**2**), Co(cob)(phen) (**3**), Cd(cob)(phen) (**4**), Mn(cob)(bpy)(H$_2$O)$_2$ (**5**), Co(cob)(bpy)(H$_2$O)$_2$ (**6**), Cu(Hcob)$_2$(bpy)(H$_2$O)$_2$·H$_2$O (**7**), Cd(cob)(bpy) (**8**) (H$_2$cob = 2−[(4'−carboxybenzyl)oxy]benzoic acid, phen = 1,10−phenanthroline, bpy = 2,2'−bipyridine) have been synthesized under hydrothermal conditions by H$_2$cob, different N−donor ligands and transition metal salts. These eight complexes have been characterized by elemental analysis, infrared (IR), thermogravimetric analysis (TGA), and single−crystal X−ray diffraction. Complexes **1**, **3** and **4** are isostructural and feature a two−dimensional (2D) wave−like layer network, which further interconnected by inter−layer π···π stacking interaction to form a three−dimensional (3D) supramolecular structures. Complex **2** and **7** are both mononulear strucures which further self−assembled through hydrogen bonding and π···π stacking interaction to generate 3D supramolecular structures. Complexes **5** and **6** are isostructural and show one−dimensional (1D) zigzag chains, which further connected by hydrogen bonding to form a 2D supramolecular structure. Complex **8** is an infinite 1D linear structure. Desorption of lattice water molecules in complexes **2**, **5** and **6** was analyzed, which demonstrates that these water molecules may influence the construction of final structures. The water sorption studies reveal that complexes **2**, **5** and **6** exhibit good water vapor uptake (64.12 ml/g for **2**, 40.26 ml/g for **5** and 55.34 ml/g for **6**). Furthermore, fluorescence properties of **1**−**8** have been investigated. Magnetic susceptibility measurements indicate that complexes **1**−**3** show weak antiferromagnetic behavior, while **5**−**6** exhibit ferromagnetic behaviors.

Introduction

Construction of hybrid metal−organic coordination polymers has been an attractive research field in crystal engineering, supramolecular, inorganic, solid and materials chemistry, which is due to their ability to form intriguing architectures and their potential applications in magnetism, catalysis, luminescence and separation.[1−5] Until now, rational design and synthesis of coordination polymers with expected structure are still challenges for researchers, and much effort has been devoted to design and synthesize complexes with unique structures and properties.[6] However, many other factors such as metal−ligand ratios, the pH value, temperature, the solvent system, auxiliary ligands, etc., also influence the final structure.[7−11] Since the structures of coordination polymers are closely related to the coordination modes of different metal centers and organic ligands, it's very important to select proper types of organic ligands containing N− and O−donors to construct novel structures.[12−13] Up to now, coordination polymers of high dimensional structures based on O−donor ligands or N−donor ligands have been mostly studied.[14−17]

Flexible dicarboxylate ligands have four potential coordination sites, which can adopt versatile coordination modes (Scheme 1). In addition, it can act as hydrogen bond donors and acceptors depending on the degree of deprotonation, which make it a wonderful candidate for the construction of many unpredictable multi−dimensional structures. Furthermore, N−donor ligands used as auxiliary ligands are also excellent candidate for the construction of novel coordination polymers, since they can provide many strong nitrogen coordination donors to the metal centres, and the pyridine rings can not only interact to each other with π···π stacking interactions, but also act as hydrogen bond donors and acceptors.[18] 2,2'−bipyridine and 1,10−phenanthroline are very similar ligands and always coordinate with metal atoms in chelating modes because of their distances between two N atoms.[19] Based on these ideas, our group tried to tune the structural dimension of coordination polymers by a flexible O−donor ligand of 2−[(4'−carboxybenzyl)oxy]benzoic acid and two rigid N−donor ligands.[20−21]

In this paper, we chose the flexible, 2−[(4'−carboxybenzyl)oxy]benzoic acid as the main ligand, 2,2'−bipyridine and 1,10−phenanthroline monohydrate as auxiliary ligands to react with different transition metal salts under hydrothermal conditions. Then eight complexes Mn(cob)(phen) (**1**), Co(cob)(phen)$_2$(H$_2$O)·5H$_2$O (**2**), Co(cob)(phen) (**3**), Cd(cob)(phen) (**4**), Mn(cob)(bpy)(H$_2$O)$_2$ (**5**), Co(cob)(bpy)(H$_2$O)$_2$ (**6**), Cu(Hcob)$_2$(bpy)(H$_2$O)$_2$·H$_2$O (**7**), Cd(cob)(bpy) (**8**) were obtained. These complexes are characterized by elemental analysis, IR, TG, and single−crystal X−ray diffraction. Fluorescence properties and magnetic properties of these materials are also discussed.

Experimental section

Materials and methods

All reagents and solvents were purchased commercially and used

as−purchased without further purification. Elemental analysis for C, H and N were carried out with a Perkin−Elmer 2400 CHN elemental analyzer. The IR spectra were recorded (as KBr pressed pellets) in the range of 400−4000 cm^{-1} on a Nicolet 170SXFT−IR spectrometer. Thermal gravimetric analysis data were collected on a Perkin−Elmer TGA 7 instrument in nitrogen at a heating rate of 10 °C/min. The PXRD diagrams were collected by a Shimadzu XRD−6000 diffractometer. Fluorescence spectra were measured by a Hitachi Model RF−5301 PC fluorescence spectrophotometer with a Xenon lamp light source. The magnetic measurements were performed on the Quantum Design SQUID MPMSXL−7 instruments in a magnetic field of 1000 Oe in the temperature range of 2−300 K.

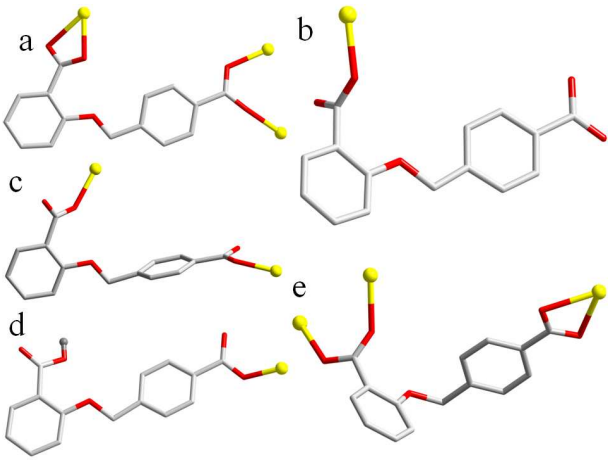

Scheme 1 Coordination modes of H_2cob ligand in complexes **1**−**8**

Synthesis of Mn(cob)(phen) (1)

A mixture of $Mn(OAc)_2{\cdot}4H_2O$ (0.1 mmol, 0.0245 g), H_2cob (0.1 mmol, 0.0272 g), phen (0.1 mmol, 0.0198 g), 25% $(C_2H_5)_4NOH$ (mass fraction) aqueous solution (0.1 ml) and H_2O (5 mL) was sealed in a 23mL Teflon−lined autoclave and heated to 110 °C for 3 days. After cooling to room temperature at a speed of 10 °C /h, yellow block crystals of complex **1** were obtained, washed with H_2O and dried in air (Yield: 45% based on Mn). Anal. Calc. for $C_{27}H_{18}MnN_2O_5$: C, 64.17; H, 3.59, N, 5.54. Found: C, 64.09; H, 3.47; N, 5.50. IR (KBr, cm^{-1}): 3381 (s), 1604 (s), 1590 (s), 1541 (s), 1515 (m), 1489 (s), 1450 (m), 1424 (s), 1409 (s), 1343 (w), 1297 (w), 1273 (w), 1247 (s), 1161 (s), 1144 (w), 1101 (m), 1046 (w), 1016 (w), 849 (w), 804 (w), 770 (m), 730 (s), 669 (q), 648 (m), 635 (w), 591 (w).

Synthesis of Co(cob)(phen)$_2$(H_2O)·5H_2O (2)

The synthetic procedure was similar to that of **1**, except that the quantity of phen is changed to 0.2 mmol. The orange block crystals were obtained, washed with H_2O and dried in air (Yield: 58% based on Co). Anal. Calc. for $C_{39}H_{38}CoN_4O_{11}$: C, 67.73; H, 4.08, N, 8.10. Found: C, 67.62; H, 4.05; N, 8.14. IR (KBr, cm^{-1}): 3381 (s), 1604 (s), 1589 (s), 1540 (s), 1515 (m), 1489 (m), 1452 (w), 1423 (m), 1409 (s), 1341 (m), 1298 (w), 1272 (w), 1246 (s), 1161 (m), 1143 (w), 1101 (m), 1045 (w), 1016 (w), 863 (s), 848 (s), 805 (w), 770 (m), 730 (s), 669(m), 648 (m), 635 (w), 592 (w).

Synthesis of Co(cob)(phen) (3)

The synthetic procedure was similar to that of **2**, except $Co(OAc)_2$ (0.1 mmol, 0.0249 g) replaced $Mn(OAc)_2{\cdot}4H_2O$. The dark−red block−like crystals were obtained, washed with H_2O and dried in air (Yield: 65% based on Co). Anal. Calc. for $C_{27}H_{18}CoN_2O_5$: C, 63.66; H, 3.56, N, 5.50. Found: C, 63.72; H, 3.34; N, 5.72. IR (KBr, cm^{-1}): 3381 (s), 1604 (s), 1590 (s), 1540 (s), 1515 (m), 1487 (s), 1452 (w), 1424 (s), 1409 (s), 1341 (w), 1298 (w), 1273 (m), 1246 (m), 1161 (w), 1143 (w), 1101 (s), 1045 (m), 1016 (w), 864 (m), 848 (s), 804 (w), 770 (m), 730 (s), 669 (m), 649 (m), 635 (w), 592 (w).

Synthesis of Cd(cob)(phen) (4)

The synthetic procedure was similar to that of **1**, except $Cd(OAc)_2$ (0.1 mmol, 0.0267 g) replaced $Mn(OAc)_2{\cdot}4H_2O$. The colorless prismatic crystals were obtained, washed with H_2O and dried in air (Yield: 63% based on Cd). Anal. Calc. for $C_{27}H_{18}CdN_2O_5$: 57.62; H, 3.22, N, 4.98. Found: C, 57.51; H, 3.34; N, 4.82. IR (KBr, cm^{-1}): 3381 (s), 1605 (s), 1589 (s), 1540 (s), 1515 (m), 1489 (m), 1452(w), 1423 (s), 1409 (s), 1341 (w), 1298 (m), 1272 (s), 1246 (m), 1161 (w), 1143 (w), 1101(m), 1047 (m), 1016 (w), 863 (m), 848 (s), 804 (w), 770 (m), 730 (s), 669 (m), 647 (w), 635 (w), 591 (w).

Synthesis of Mn(cob)(bpy)(H_2O)$_2$ (5)

The synthetic procedure was similar to that of **1**, except bpy (0.1 mmol, 0.0156 g) replaced phen. The yellow block crystals were obtained, washed with H_2O and dried in air (Yield: 42% based on Mn). Anal. Calc. for $C_{25}H_{22}MnN_2O_7$: C, 58.04; H, 4.29; N, 5.41. Found: C, 58.15; H, 4.44; N, 5.42. IR (KBr, cm^{-1}): 3381 (s), 1604 (s), 1588 (s), 1540 (s), 1515 (m), 1489 (m), 1451 (w), 1426 (s), 1409 (s), 1341 (w), 1296 (w), 1273 (w), 1246 (m), 1161 (w), 1143 (w), 1100 (m), 1045 (w), 1016 (w), 863 (m), 848 (s), 804 (w), 770 (m), 730 (s), 670(m), 648.25 (m), 635 (w), 592 (w).

Synthesis of Co(cob)(bpy)(H_2O)$_2$ (6)

The synthetic procedure was similar to that of **5**, except $Co(OAc)_2$ (0.1 mmol, 0.0249 g) replaced $Mn(OAc)_2{\cdot}4H_2O$. The dark−red block crystals were obtained, washed with H_2O and dried in air (Yield: 55% based on Co). Anal. Calc. for $C_{25}H_{22}CoN_2O_7$: C, 57.59; H, 4.25; N, 5.37. Found: C, 57.54; H, 4.24; N, 5.40. IR (KBr, cm^{-1}): 3381 (s), 1604 (s), 1589 (s), 1540 (s), 1515 (m), 1489 (s), 1452(m), 1422 (s), 1410 (s), 1342(w), 1298 (w), 1272 (w), 1245 (m), 1161 (m), 1143 (w), 1102 (w), 1045 (w), 1016 (w), 863 (w), 848 (m), 804 (w), 770 (m), 730 (w), 669 (m), 648 (m), 636 (w), 592 (w).

Synthesis of Cu(Hcob)$_2$(bpy)(H_2O)$_2$·H_2O (7)

The synthetic procedure was similar to that of **5**, except $Cu(OAc)_2$ (0.1 mmol, 0.0200 g) replaced $Mn(OAc)_2{\cdot}4H_2O$. The dark−blue block crystals were obtained, washed with H_2O and dried in air (Yield: 21% based on Cu). Anal. Calc. for $C_{40}H_{34}CuN_2O_{12}$: C, 60.71; H, 5.48; N, 3.54. Found: C, 60.77; H, 5.45; N, 3.47. IR (KBr, cm^{-1}): 3381 (s), 1605 (s), 1589 (s), 1540 (s), 1515 (m), 1489 (w), 1451 (m), 1423 (s), 1409 (s), 1298 (w), 1246 (s), 1161 (s), 1143 (w), 1272 (m), 1101 (m), 1045 (w), 1016 (w), 848 (s), 804 (w), 770 (m), 731 (m), 669 (m), 650 (w), 638 (w), 592 (w).

Synthesis of Cd(cob)(bpy)(8)

The synthetic procedure was similar to that of **5**, except

$Cd(OAc)_2$ (0.1 mmol, 0.0267 g) replaced $Mn(OAc)_2{\cdot}4H_2O$. The colorless block crystals were obtained, washed with H_2O and dried in air (Yield: 57% based on Cd). Anal. Calc. for $C_{25}H_{18}CdN_2O_5$: C, 55.726; H, 3.37; N, 5.20. Found: C, 55.76; H, 3.29; N, 5.15. IR (KBr, cm^{-1}): 3381 (s), 1606 (s), 1591 (s), 1540 (s), 1515 (m), 1489 (s), 1452(w), 1424 (s), 1410 (s), 1341 (w), 1298 (w), 1272 (w), 1246 (m), 1161 (s), 1143 (w), 1100 (m), 1045 (w), 1016 (w), 863 (w), 850 (s), 805 (w), 770 (s), 730 (s), 669 (m), 650 (w), 635 (w), 591 (w).

Single−crystal X−ray crystallography

Diffraction data for **1**−**8** were collected on a Bruker Smart Apex CCD diffractometer by graphite−monochromated Mo−Kα radiation (λ = 0.71073 Å). Empirical absorption corrections were taken from SADABS.[22] The space group was determined by using XPREP.[23] The structures were solved by direct methods and refined on F^2 with full−matrix least−squares method using the SHELXS−97 and SHELXL−97.[24] The crystallographic data for complexes **1**−**8** were summarized in Table 1. Selected bond lengths and angles are given in Table S1, ESI. Hydrogen bonding interactions of **1**−**8** are given in Table S2, ESI.

Table 1. Crystal and X−ray experimental data for **1**−**8**.

Complex	**1**	**2**	**3**	**4**
Empirical formula	$C_{27}H_{18}MnN_2O_5$	$C_{39}H_{38}CoN_4O_{11}$	$C_{27}H_{18}CoN_2O_5$	$C_{27}H_{18}CdN_2O_5$
Formula weight	505.37	797.66	509.36	562.83
Crystal system	Monoclinic	Triclinic	Monoclinic	Monoclinic
Space group	*C2/c*	*P−1*	*C2/c*	*C2/c*
a(Å)	19.0671(19)	10.7055(7)	19.0329(18)	19.2419(7)
b(Å)	10.4052(8)	12.5640(9)	10.3950(9)	10.4225(3)
c(Å)	22.3840(19)	15.7296(10)	22.382(2)	22.3595(7)
α(°)	90	113.095(2)	90	90
β(°)	99.0040(10)	98.8500(10)	99.0210(10)	98.6760(10)
γ(°)	90	102.2290(10)	90	90
V(Å ^{3})	4386.2(7)	1834.7(2)	4373.5(7)	4432.9(2)
Z	8	2	8	8
Temperature (K)	293(2)	293(2)	293(2)	293(2)
D (Mg/m^3)	1.531	1.444	1.547	1.687
μ (mm^{-1})	0.646	0.536	0.829	1.029
F (000)	2072	830	2088	2256
$R_1(I>2\sigma(I))$	0.0460	0.0590	0.0593	0.0376
R_1(all data)	0.0745	0.0918	0.1072	0.0601
w$R_2(I>2\sigma(I))$	0.0929	0.1455	0.1441	0.0652
wR_2(all data)	0.1105	0.1686	0.1803	0.0764
GOF on F^2	1.030	1.029	1.044	1.064
	5	**6**	**7**	**8**
Empirical formula	$C_{25}H_{22}MnN_2O_7$	$C_{25}H_{22}CoN_2O_7$	$C_{40}H_{34}CuN_2O_{12}$	$C_{25}H_{18}CdN_2O_5$
Formula weight	517.39	521.38	798.24	1077.63
Crystal system	Monoclinic	Monoclinic	Triclinic	Monoclinic
Space group	*C2/c*	*C2/c*	*P−1*	*C2/c*
a(Å)	35.130(3)	35.083(3)	7.5718(7)	12.6755(5)
b(Å)	7.3946(3)	7.2940(5)	14.0421(19)	16.9830(6)
c(Å)	19.1657(13)	19.1329(17)	17.244(2)	20.7087(11)
α(°)	90	90	74.5340(10)	90
β(°)	109.809(2)	109.888(2)	83.8040(10)	103.418(2)
γ(°)	90	90	88.439(2)	90
V(Å ^{3})	4684.1(5)	4604.0(6)	1756.7(4)	4336.2(3)
Z	8	8	2	4
Temperature (K)	293(2)	293(2)	293(2)	293(2)
D (Mg/m^3)	1.467	1.504	1.509	1.651
μ (mm^{-1})	0.613	0.795	0.693	1.048
F (000)	2136	2152	826	2160
$R_1(I>2\sigma(I))$	0.0567	0.0572	0.0690	0.0358
R_1(all data)	0.1107	0.1128	0.1358	0.0597
w$R_2(I>2\sigma(I))$	0.0879	0.1147	0.0796	0.0572
wR_2(all data)	0.1150	0.1421	0.1025	0.0667
GOF on F^2	1.057	0.991	1.095	1.040

Results and discussion

Synthesis

Complexes **1**, **3** and **4** reported here were obtained by the

combination of H_2cob, phen and three different transition metal salts under hydrothermal conditions, showing an isostructural structure. The mole ratio of H_2cob, phen and three different transition metal salts is 1:1:1. If the mole ratio of H_2cob, phen and transition metal salts was changed to 1:2:1, a different structure of Co containing complex **2** was obtained. Complexes **5**−**8** were obtained by the combination of H_2cob, bpy and four different transition metal salts with the mole ratio of 1:1:1 under hydrothermal conditions, showing three different structures. In addition, auxiliary ligands and different coordination mode of cob^{2-} ligand may play important roles in complexes **1**−**8**, which may be a feasible method to adopt different ligands to construct coordination polymers with target structures.

Crystal Structure of complex 1

Single crystal X−ray analysis reveals that complexes **1, 3** and **4** are isomorphous and crystallize in the monoclinic space group of *C2/c*. Thus, only the crystal structure of complex **1** will be described as a representative example here. The asymmetric unit of **1** is composed of one Mn(II), one cob^{2-} and one phen. As shown in Figure S1, the Mn(II) atom in **1** adopts a distorted octahedral coordination geometry formed by four O donors from three cob^{2-} ligands and two N donor from one phen ligand. The O2 and O1 atoms are disordered in the final structure. The Mn−O bond lengths range from 2.086 to 2.452 Å, and the Mn−N bond lengths are 2.322 and 2.335 Å (Table S1). In complex **1**, the carboxyl groups of the cob^{2-} ligands are all deprotonated, exhibiting bidentate/bridging coordination mode, as shown in Scheme 1a. One carboxyl group (O1−C1−O2) coordinates to one Mn(II) atom through bidentate mode, and the other one (O3−C8−O4) serves as a bridge to connect two Mn(II) atoms. The Mn1 centers are connected by these two types of carboxyl groups to form a 2D wave−like layer network along *c* axis (Fig. 1). The cob^{2-} ligand presents a dihedral angle of 5.59° between the two benzene rings, which is nearly parallel. The chelating phen ligand occupies two coordination sites of Mn(II) atom, terminates one possible dimension for connectivity reducing the latter to high dimensional structure.

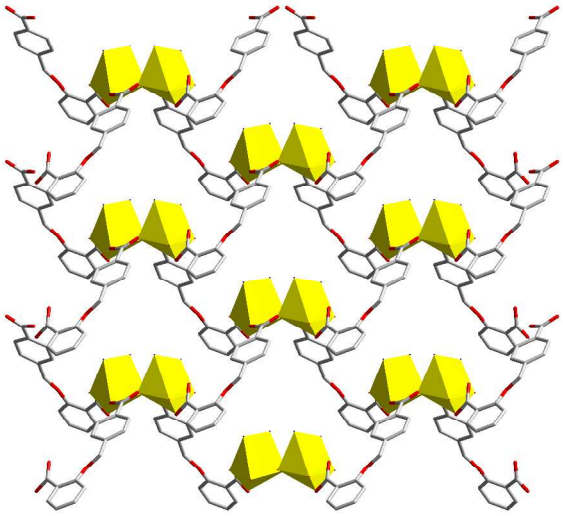

Fig. 1 The 2D wave−like layer of **1**, viewed along the *c* axis (phen ligands are omitted for clarity).

Based on these connection modes, the cob^{2-} ligands can be regarded as 3−connected nodes to link three Mn(II). The six−coordinated Mn(II) atoms can be considered as 3−connected nodes linked by three cob^{2-} ligands to form a (3, 3) net (Fig. 2). There are π···π stacking interactions between the nearly parallel cob^{2-} ligands with the distances between planes of cob^{2-} from 3.7168 to 3.8779 Å. Thus, the 2D network is extended to a 3D supromolecular architecture by π···π stacking interactions along *a* axis. Undoubtedly, the π···π stacking interactions play important roles in the stabilization of the supramolecular architectures (Figure S2).

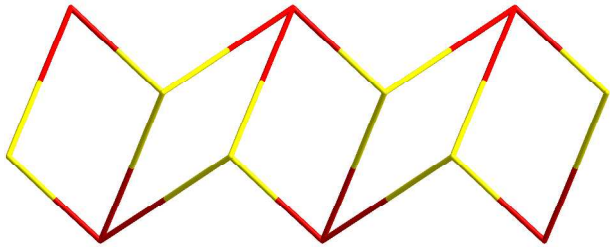

Fig. 2 Schematic illustrating the 2D network of complex **1**. Color code: yellow, Mn, cob^{2-} ligand: red.

Crystal Structure of complex 2

Complex **2** shows a mononuclear structure, and crystallizes in the triclinic space group of *P−1*. The asymmetric unit contains one Co(II) atom, one cob^{2-} ligand, two phen ligands, one coordinated water molecule and five lattice water molecules. The Co(II) atom is six−coordinated by two O donors from one cob^{2-} ligand with one coordinated water molecule and four N donors from two chelating phen ligands in a distorted octahedral coordination geometry (Figure S3). In **2**, only one carboxyl group of the cob^{2-} ligand participates in bonding while the other one remains free satisfying the charge of the metal centers, exhibiting another coordination mode (Scheme 1b). Unlike **1**, there are two chelating phen ligands in each asymmetric unit, which occupies four coordination sites of Co(II) atom. The chelating phen ligands terminate two possible dimensions, which may reduce the complex to high dimensional network.

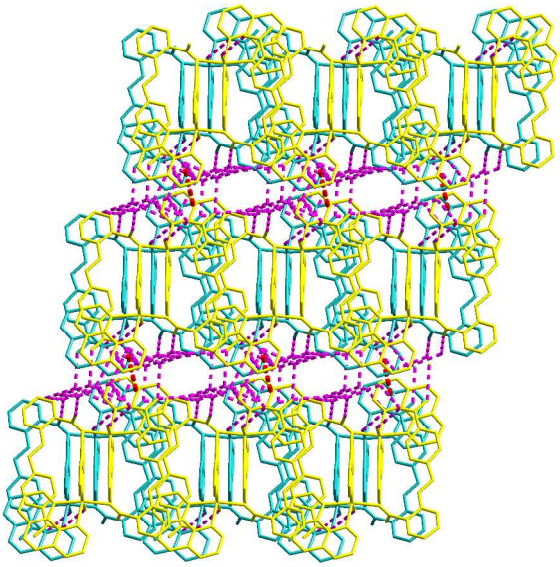

Fig. 3 3D supramolecular structure of **2** constructed by hydrogen bonding and π···π stacking interactions along *b* axis. (pink lines: hydrogen bond;

red lines: π···π stacking interactions turquoise and yellow represent three 2D supramolecular layer, respectively)

Notably, significant intermolecular hydrogen bonding interactions exist in complex **2** (Table S2). The monomers of complex **2** are connected together into a supramolecular dimer cage by hydrogen bonding between the uncoordinated O3 atom of the carboxyl group of cob^{2-} ligand and the O6 atom of the coordinated water molecule (Figure S4). The Co···Co and O···O distance are 8.478 and 2.630 Å, respectively. The dimer are further linked by the hydrogen bonding among the uncoordinated oxygen atoms of the carboxyl group and the oxygen atoms of the lattice water molecules to form a 1D supramolecular chain along *b* axis (Figure S5). The hydrogen bonding between the uncoordinated O4 atom of the carboxyl group and the O9 atom of the lattice water molecule further connects 1D supramolecular chain to form a 2D layer along *a* axis (Figure S6). Finally, the π···π stacking interactions between the nearly phen ligands with the distances between 3.6499 Å to 3.8356 Å connect the adjacent 2D layer to a 3D supramolecular structures along *c* axis (Fig. 3).

Crystal Structure of complex 5

As the single crystal X−ray diffraction analysis reveals that complex **5** and **6** are isostructural, thus only complex **5** is described in detail. Complex **5** is a zigzag 1D coordination chain and crystallizes in the monoclinic space group of *C2/c*. In the asymmetric unit of complex **5**, there are one Mn(II) atom, one cob^{2-} ligand, one bpy ligand and two coordinated water molecules. The Mn(II) atom is six−coordinated by four O donors from two different cob^{2-} ligands with two coordinated water molecules and two N donors from one chelating bpy ligand to form a distorted octahedral coordination geometry (Figure S7). The cob^{2-} ligand in complex **5** adopts a bridging coordination mode to connect two Mn(II) atoms (Scheme 1c), linking the Mn(II) atoms into an infinite 1D zigzag chain with a Mn···Mn distance of 10.3697 Å (Fig. 4). The cob^{2-} ligand presents a dihedral angle of 83.73° between the two benzene rings, which is nearly vertical

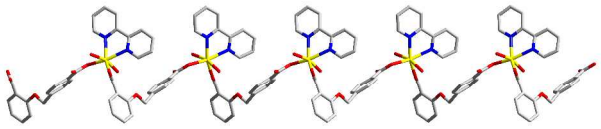

Fig. 4 1D zigzag chain of complex **5**, viewed along the *b* axis, hydrogen atoms are omitted for clarity.

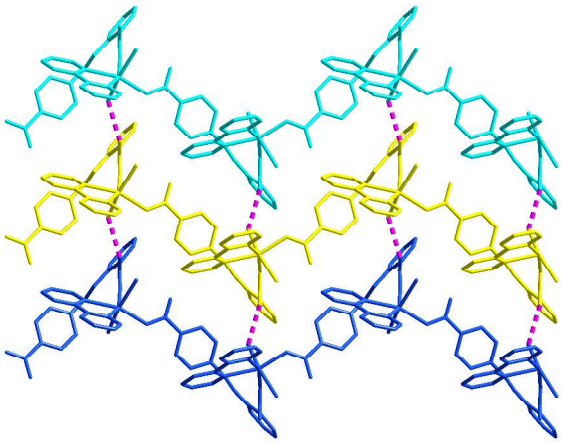

Fig. 5 2D supramolecular layer formed by hydrogen bonding along *b* axis. (pink lines: hydrogen bond; turquiose, yellow and light blue represent three 1D supramolecular chains, respectively)

Similarly to complex **1**, the bpy ligands and two coordinated water molecules terminate the chains on each side preventing the linkage between the chains into high dimension structure. The adjacent 1D chains are held together through the hydrogen bonding (O7−H7···O2) through the uncoordinated O2 atom of the carboxyl group, forming a 2D ladder−like supramolecular layer (Fig. 5, Table S2).

Crystal Structure of complex 7

Single crystal X−ray diffraction analysis shows that complex **7** crystallizes in the triclinic space group of *P−1*, and each asymmetric unit consists one Cu(II) atom, two cob^{2-} ligands, one bpy ligand, one coordinated water molecule and one lattice water molecule. As shown in Figure S8, the Cu(II) atom is five−coordinated and described as a slightly distorted tetrahedron coordination geometry: two bridging oxygen atom from two different $Hcob^{-}$ ligand, two nitrogen atoms from one bpy ligand and one coordinated water molecule. Different from the complexes above, the $Hcob^{-}$ ligand is partially deprotonated, and only one carboxyl group can bridge to the Cu(II) atom (Scheme 1d).

The monomers of complex **7** self−assemble via intermolecular hydrogen bonding interactions to form 1D linear chains (Figure S9). Theses chains are further connected by interchain hydrogen bonding interactions leading to a 2D supramolucular structure (Figure S10). The representative intermolecular hydrogen bonding lengths are listed in Table S2. Finally, these 2D layer are linked by the π···π stacking interactions between the nearly bpy ligands with the distances between 3.5721 to 3.9075 Å to form a 3D supramolecular structure (Fig. 6).

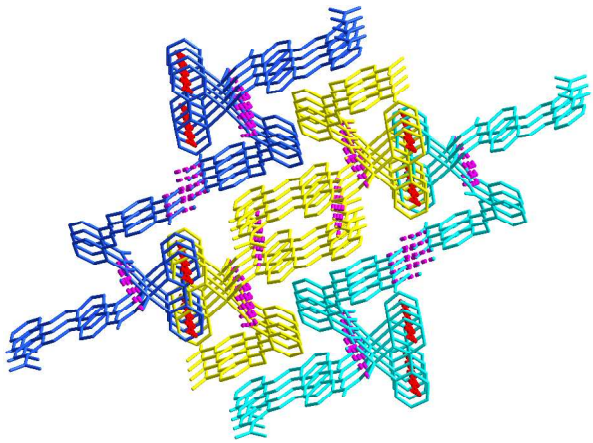

Fig. 6 3D supramolecular structure of **7** constructed by hydrogen bonding and π···π stacking interactions. (pink lines: hydrogen bond; red lines: π···π stacking interactions; turquiose, yellow and light blue represent three 2D supramolecular layers, respectively)

Crystal Structure of complex 8

Single−crystal X−ray analysis of **8** exhibits a 1D linear structure, crystallizing in the monoclinic space group of *C*2/c. The asymmetric unit contains one Cd(II) atom, one cob^{2-} ligand and one bpy ligand. As shown in Figure S11, each Cd(II) atom is six−coordinated to four O donors of two carboxylate groups from two different cob^{2-} ligands and two N donors of one bpy ligand in

a distorted octahedral coordination geometry. In **8**, the fully deprotonated cob^{2-} ligand connects two Cd(II) atoms to an infinite 1D linear structure along the *c* axis (Fig. 7 , Scheme 1e). Compared to the coordination modes of the cob^{2-} ligand in **1**−**7**, the two carboxyl groups chelate two different Cd(II) atoms and the chelating bpy ligands terminate to the Cd(II) atoms, which prevent further expansion of the whole structure. The cob^{2-} ligand presents a nearly vertical dihedral angle of 85.03° between the two benzene rings.

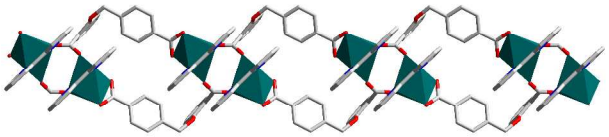

Fig. 7 1D zigzag chain of complex **8**, viewed along the *b* axis, hydrogen atoms are omitted for clarity.

The effects of coordination modes of H_2cob ligand and N−donor ligands on the final structures of complexes

In order to explore the effect of the mixed O−donor and N−donor ligands on the design of low dimensional structures, complexes **1**−**8** were synthesized hydrothermally by using the flexible dicarboxylate H_2cob ligand as the main ligand, two N−donor ligands as the auxiliary ligands and four transition metal salts under the mostly same condition. The resulting structures of **1**−**8** appear to be affected by two main features: coordination modes of the carboxyl groups of H_2cob ligands and N−donor ligands. According to the different structures discussed above, the cob^{2-} ligands connect the metal atoms in five types of coordination modes (Scheme 1). For complexes **1**, **3** and **4**, the cob^{2-} ligand exhibits both bridging and chelating mode, displaying a 2D architecture. The chelating phen ligand occupies two coordination sites of Mn(II) atom, terminates one possible dimension for connectivity reducing the latter to high dimensional structure. We try to double the quantity of the phen ligand, and obtained a mononuclear structure of complex **2** as expected. There are two chelating phen ligands in each asymmetric unit, which may reduce the complex to high dimensional network. In addition, one carboxyl group of cob^{2-} ligand in **2** is not coordinated, and the other one bridges one Co center to a mononuclear structure (Scheme 1b). In complexes **5** and **6**, both carboxyl groups of the cob^{2-} ligands bridge two Co(II) atoms in an monodentated coordination mode, resulting in a 1D zigzag chain (Scheme 1c). The bpy ligands and two coordinated water molecules terminate the Co(II) atoms on each side preventing the linkage between the chains into high dimension structure. Because of the flexibility of the cob^{2-} ligand, the dihedral angle of the two benzene rings of the cob^{2-} ligand in **5** is 83.73° comparing with the dihedral angle of 5.59° in complex **1**. The nearly vertical angle may further present the chains into high dimensional structure. The coordination mode in complex **7** is similar to that in complex **2**. The difference is that the other carboxyl group doesn't participate in coordination since it is undeprotonated. In complexes **8**, both carboxyl groups of the cob^{2-} ligands and bpy ligands connect the Cd(II) atoms in a chelating mode, generating a 1D chain. In these manners, the auxiliary N−donor ligands and different coordination modes of the cob^{2-} ligands may have a remarkable effect on the structures of the complexes. It is a possible method to tune the different structural dimensions by introducing different ligands with various coordination modes.

The effects of lattice water molecules on the structures of complexes 2, 5 and 6

Desorption of lattice water molecules of complexes **2**, **5** and **6** was analyzed. Therefore, crystals of **2**, **5** and **6** were soaked in dichloromethane (CH_2Cl_2) for 48h and afterward PXRD analyses were performed (Fig. S39−S41). According to the obviously changed PXRD patterns, the peaks of the CH_2Cl_2−exchanged samples are quite different from before, which suggest that the removal of the lattice molecules triggers the structural change and influence the structural construction. Additional gas sorption experiment was also performed (ESI).

Thermogravimetric analysis

To study the thermal stabilities of complexes **1**–**8**, TGA was performed in the temperature of 30−600 °C (see Fig. 8). There is no obvious weight loss before 320 °C for complex **1** and then it decomposes rapidly on further heating. For complex **2**, the weight loss from 33−140 °C is consistent with the removal of one coordinated water molecule and five lattice water molecules (calculated: 13.55%, found: 12.65%), and the residual complex begins to decompose at 260 °C. A total loss of Complex **5** lost % is observed for complex **6** from room temperature to °C, which is due to the loss of two coordinated water molecules. Upon further heating, rapid weight loss occurs owing to the decomposition of the complex. Complex **3** and **4** remain stability up to 150°C and 340°C, and then start to decompose. For **5** and **6**, weight losses of 7.03% and 6.95% were observed in the temperature range of 33−137°C and 33−120 °C, respectively, corresponding to the loss of two coordinated water molecules (calculated: 6.96% and 6.91%, respectively). The residual complexes begin to decompose at 225 °C and 280 °C, respectively. For complex **7**, the TGA curve shows the weight loss of 5.88 % from 33−172 °C can be attributed to the removal of two coordinated water molecules and one lattice water molecule (calculated 6.23%) and then the framework undergoes decomposition after 225 °C. Complex **8** is stable up to 298 °C and then decomposes rapidly.

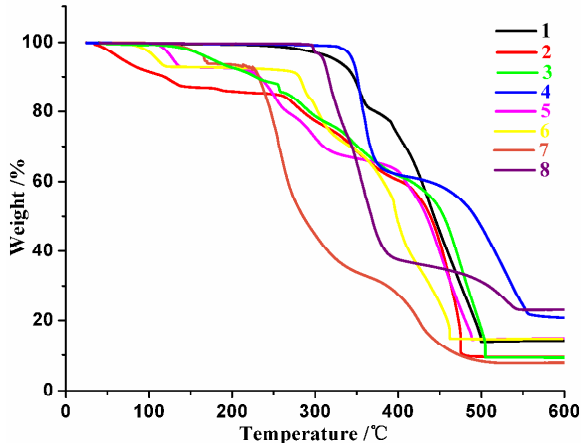

Fig. 8 TG curves for complexes **1**−**8.**

Fluorescence properties

The solid−state emission spectra of complexes **1**−**8** with H_2cob and two N−donor ligands have been investigated at room temperature. As shown in Figure S23−S30, the main emission

peaks of the H_2cob, 2,2'−bipy and 1,10−phen ligands are at 360, 390, 379 nm (λ_{ex} = 250 nm), respectively, which may be attributed to the π*−π or π*−n transitions of the intraligands.[25] Upon excitation of solid samples of **1**−**8** at 270 nm, these complexes show emissions bands with maximum at 358 nm for **1**, 369 nm for **2**, 385 nm for **3**, 373 nm for **4**, 380 nm for **5**, 400 nm for **6**, 351 nm for **7**, and 389 nm for **8**, respectively. The emissions of **1**−**8** may be assigned to intraligand transition upon the complexation of the mixed ligands with metal ions.[26] In addition, the emissions of complexes of **1**−**3** and **5**−**7** may be attributed to the metal−ligand charge transfer, while the emissions of complexes of **4** and **8** may be caused by the ligand to metal charge transfer. Comparing with the emission of the free ligands, the different red or blue shifts and intensities of the emission peaks of these complexes were observed, which may be assigned to the differences of the coordination environment and the different structure because the photoluminescence behavior is closely associated with the coordinated ligands and metal ions.[27]

Water vapor sorption of complexes 2, 5 and 6

From the TGA studies, it seems that the solvent molecules could be removed by heating the samples above 110 °C. Thus, we measured the water vapor sorption behaviour of complexes **2**, **5** and **6**. Before the measurements, the samples of these complexes were heated at 110 °C for 12 h under vacuum to remove the guest molecules trapped inside the pore. Water vapor sorption isotherms at 298 K are presented in Fig. 9. All these complexes exhibited gradual uptakes of water reaching a maximum value of 64.12 ml/g (**2**), 40.26 ml/g (**5**) and 55.34 ml/g (**6**) at P/P_0 = 0.95 (P_0 is the saturation pressure of H_2O at 298K), respectively. The obvious hysteresis of the desorption isotherms of all the complexes may suggest that the water molecules are strongly adsorbed in the pores of these complexes, which plausibly due to the hydrogen bonding interactions in the structure.

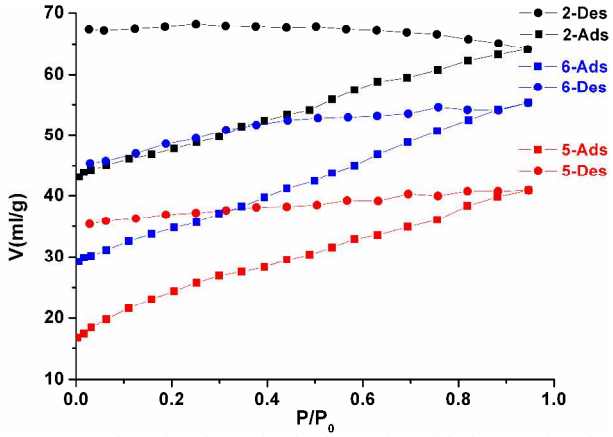

Fig. 9 Water adsorption-desorption isotherms for 2 (black), 5 (red) and 6 (blue) at 298 K.

Magnetic properties for complexes 1, 2, 3, 5, 6

The magnetic properties of complexes **1**, **2**, **3**, **5** and **6** were investigated over the temperature range of 2−300K at an applied field of 1000 Oe. The magnetic behavior of complex **1** was shown as plots of the product $1/\chi_m$ versus T and $\chi_m T$ versus T in Fig. 10. The $1/\chi_m$ versus T plot for **1** displays Curie−Weiss behavior from 300 to 20 K, and the best linear fit of $\chi_m^{-1}(T)$ data above 20 K yields C = 4.48 cm^3 K mol^{-1} and θ = −1.40 K. This negative Weiss constant indicated the presence of a very weak antiferromagnetic interaction between spin centres. The $\chi_m T$ value of **1** at 300 K is ca. 4.47 cm^3 K mol^{-1}, which is close to the expected spin−only value for one isolated Mn(II) ions (expected $\chi_m T$ = 4.38 cm^3 K mol^{-1} per Mn(II) with g = 2.00 and S = 5/2). The value of $\chi_m T$ remains almost constant as the temperature is decreased until 70 K, followed a slow decrease to a value of 4.17 cm^3 K mol^{-1} at 20 K, and then drops sharply to a minimum value of 1.98 cm^3 K mol^{-1} at 2 K. This behavior is indicative of the occurrence of weak antiferromagnetic interactions between the Mn(II) ions in **1**. For complex **5**, the $\chi_m T$ value of **5** at 300 K is ca. 4.26 cm^3 K mol^{-1}, which is close to the expected spin−only value for one isolated Mn(II) ions (Fig. 11). Unexpectedly, the magnetic behavior of complex **5**, which are similar to that of complex **1** in mononuclear Mn(II) octahedral coordination, appears in an apparent occurrence of ferromagnetic interaction at temperature ranging from 58K to 300K. The $1/\chi_m$ versus T plot for **5** displays Curie−Weiss behavior from 300 to 50 K, the best linear fit of $\chi_m^{-1}(T)$ data above 50 K yields C = 4.24 cm^3 K mol^{-1} and θ = 3.26 K. This positive Weiss constant indicated the presence of a ferromagnetic interaction between Mn(II) centres. Although some Mn(II) complexes bridged by alkoxo or phenoxo−oxygen atoms showed ferromagnetic interactions,[28] the occurrence of ferromagnetic interactions in complex **5** remains an unclear reason.

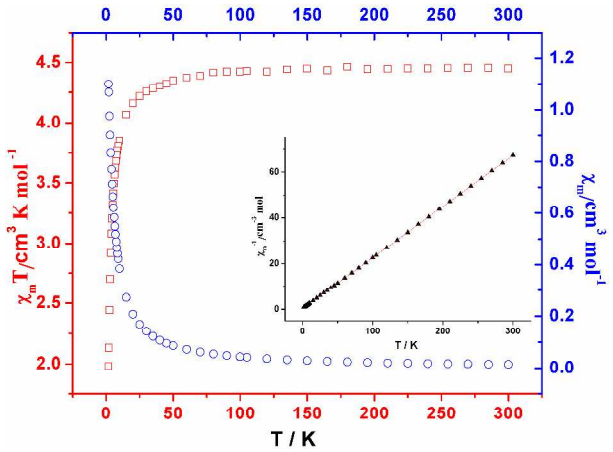

Fig. 10 Temperature dependence of magnetic susceptibilities in the form of the χ_m and χ_mT versus T for **1** at 1000 Oe. Inset: χ_m^{-1} versus T; the solid line is fit to the experimental data.

For complex **2**, the $\chi_m T$ value at 300 K is 2.56 cm^3 K mol^{-1}, which falls into a reasonable range for complexes with octahedrally coordinated Co(II) centers in the high−spin state, but is much larger than the spin−only value 1.87 cm^3 K mol^{-1} expected for the isolated high−spin Co(II) (S = 3/2 and g = 2.0). Such a magnetic behavior should result from a significant first−order orbital contribution to the magnetic moment typical of the $^4T_{1g}$ ground state of Co(II). As shown in Fig. S31, the $1/\chi_m$ versus T plot for **2** displays Curie−Weiss behavior from 300 to 50 K, the best linear fit of $\chi_m^{-1}(T)$ data above 50 K yields C = 2.66 cm^3 K mol^{-1} and θ = −5.02 K. This negative Weiss constant indicated the presence of an antiferromagnetic interaction between Co(II) centers through the intermolecular interactions. Finally, the $\chi_m T$ value decreases gradually with temperature to a minimum value of 1.75 cm^3 K mol^{-1} at 2 K. The quick low−temperature decrease in $\chi_m T$ is due to the combined

influence of a large zero−field splitting, spin–orbit coupling and somewhat antiferromagnetic interaction between Co(II) centers through the intermolecular interactions. The magnetic properties of complexs **3** in mononuclear Co(II) octahedral coordination, which are similar to that of complex **2**, are dominated by the expected significant orbital contribution to the magnetic moment and somewhat antiferromagnetic interaction between Co(II) centers by the intermolecular interactions through the two−dimensional layers or one−dimensional chains. Because the best linear fit of $\chi_m^{-1}(T)$ data by Curie−Weiss law above 50 K yields θ = −6.68 K for **3** (Fig. S32). For complex **6**, however, upon cooling the $\chi_m T$ value exhibits a slight increase until 120 K; this may be indicative of the occurrence of weak ferromagnetic interactions between Co(II) centers through the intermolecular interactions. As shown in Fig. S33, the inverse molar susceptibility above 50 K fits well with the Curie–Weiss law with a Curie constant C = 3.18 cm^3 K mol^{-1} and a Weiss temperature θ = 2.95 K. The positive Weiss constant indicated ferromagnetic coupling between the Co(II) ions. The quick low−temperature decrease in $\chi_m T$ also results from the influence of a large zero−field splitting, a combined effect of the local distortion of the octahedral crystal−field and spin–orbit coupling.

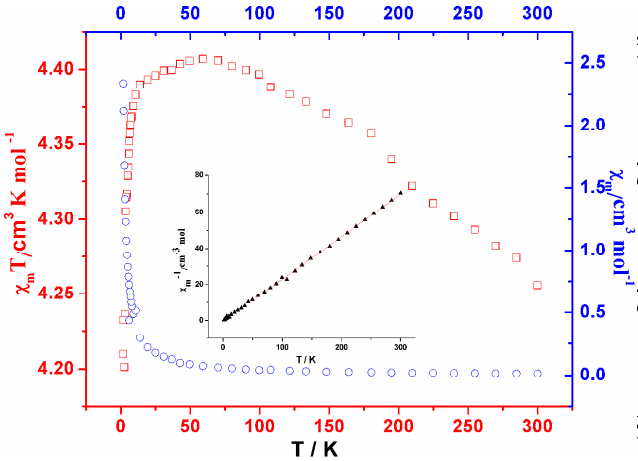

Fig. 11 Temperature dependence of magnetic susceptibilities in the form of the χ_m and χ_mT versus T for **5** at 1000 Oe. Inset: χ_m^{-1} versus T; the solid line is fit to the experimental data.

Conclusions

In summary, eight coordination polymers based on flexible H_2cob ligand and two N−donor ligands have been synthesized under hydrothermal conditions. According to the structures of these eight complexes, we have found that the final architecture can be influenced by the coordination mode of H_2cob ligand, the mole ratio of reactants and the auxiliary N−donor ligands. In addition, complexes **1**−**7** are strengthened by the hydrogen bonding or π···π stacking interactions. The photoluminescent behaviors indicate that different red or blue shifts and intensities of the emission peaks of these complexes were observed, which may be good optical materials. Complexes **2**, **5** and **6** show good water vapor uptake. Magnetic susceptibility measurements indicate that complex **1**−**3** exhibit antiferromagnetic coupling and complexes **5**−**6** show ferromagnetic behaviors which can be foreseen as magnetic materials. This work evidently indicates that the effect of auxiliary ligands and coordination modes of H_2cob are critical in construction of polymeric arrangement. Subsequent studies will be focused on the structures and properties of a series of coordination complexes constructed by mixed ligands with aromatic dicarboxylate ligands and N−donor ligands.

Acknowledgment

This work was financially supported by the National Nature Science Foundation of China (No. 21271024 and 20971014), supported by Beijing Natural Science (No 2112037), Foundation the 111 Project (B07012) in China, Foundation of the Open Project of Key Laboratory of Polyoxometalates Science of Ministry of Education of Northeast Normal University.

Notes and references

Key Laboratory of Cluster Science of Ministry of Education, School of Chemistry, Beijing Institute of Technology, Beijing 100081, PR China
E−mail: huangrudan1@bit.edu.cn

† Electronic Supplementary Information (ESI) available: X−ray crystallographic cif files, additional structural discription of complexes **1**−**8**, selected bond lengths and angles and simulated and measured XRPD patterns, discription of gas sorption and PXRD of CH_2Cl_2−exchanged samples about complexes **2**, **5** and **6**. Complexes **1**−**8** have been assigned the following numbers: CCDC 967260, 967261, 967258, 967262, 967263, 967259, 967264 and 967257.

1 (a) C. Y. Jiang, T. Wu, S. T. Zheng, X. Zhao, Q. P. Lin, X. H. Bu, P. Y. Feng, *Cryst, Growth. Des.*, 2011, **11**, 3713; (b) Z. Y. Guo, H. Wu, G. Srinivas, Y. M. Zhou, S. C. Xiang, Z. X. Chen, Y. T. Yang, W. Zhou, M. O'Keeffe, B. L. Chen, *Angew. Chem. Int. Ed.*, 2011, **50**, 3178; (c) J. R. Li, H. C. Zhou, *Nature Chemistry,* 2010, **2**, 893; (d) Q. L. Zhu, W. Chu, R. D. Huang, L. J. Dong, X. Y. Cao, C. W. Hu, *Inorg. Chem. Commun.*, 2010, **13**, 1459; (e) R. B. Getman, Y. S. Bae, C. E. Wilmer, R. Q. Snurr, *Chem. Rev.*, 2012, **112** , 703.

2 (a) J. L. Zhang, H. Ji, Y. G. Wei, Y. Wang, N. Z. Wu, *J. Phys. Chem. C.*, 2008, **112**, 10688; (b) L. J. Dong, X. F. Li, J. Cao, W. Chu, R. D. Huang, *Dalton. Trans.*, 2012, **42**, 1342.

3 (a) F. J. Song, C. Wang, W. L. Lin, *Chem. Commun.*, 2011, **29**, 8256; (b) C. C. Ji, L. Qin, Y. Z. Li, Z. J. Guo and H. G. Zheng, *Cryst. Growth Des.*, 2011, **11**, 480; (c) M. Yoon, R. Srirambalaji, K. Kim, *Chem. Rev.*, 2012, **112**, 1196; (d) J. A. Perman and M. J. Zaworotko, *J. Chem. Crystallogr.*, 2008, **39**, 78; (e) X. N. Cheng, W. X. Zhang and X. M. Chen, *J. Am. Chem. Soc.*, 2007, **129**, 15738; (f) N. D. Schley, J. D. Blakemore, N. K. Subbaiyan, C. D. Incarvito, F. D'Souza, R. H. Crabtree, G. W. Brudvig, *J. Am. Chem. Soc.*, 2011, **133**, 10473.

4 (a) M. Hashimoto, S. Igawa, M. Yashima, I. Kawata, M. Hoshino, M. Osawa, *J. Am. Chem. Soc*., 2011, **133**, 10348; (b) L. J. Dong, W. Chu, Q. L. Zhu, R. D. Huang, *Cryst. Growth Des.*, 2011, **1**, 93; (c) C. A. Kent, D. Liu, T. J. Meyer, W. Lin, *J. Am. Chem. Soc.*, 2012, **134**, 3991.

5 (a) D. Banerjee, S. J. Kim, W. Li, H. H. Wu, J. Li, L. A. Borkowski, B. L. Philips, J. B. Parise, *Cryst. Growth Des.*, 2010, **10**, 2801; (b) J. R. Li, J. Sculley, H. C. Zhou, *Chem. Rev.*, 2012, **112**, 869; (c) M. Padmanaban, P. Muller, C. Lieder, K. Gedrich, R. Grunker, V. Bon, I. Senkovska, S. Baumgartner, S. Opelt, S. Paasch, E. Brunner, F. Glorius, E. Klemm, S. Kaskel, *Chem. Commun.*, 2011, **47**, 12089; (d) S. Kitagawa, R. Kitaura and S. Noro, *Angew. Chem., Int. Ed.*, 2004, **43**, 2334; (e) X. J. Cao, J. Zhang, C. J. Wang, Y. Y. Zhu and G. Li, *CrystEngComm,* 2012, **14**, 4357.

6 (a) J. J. Perry IV, J. A. Perman and M. J. Zaworotko, *Chem. Soc. Rev.*, 2009, **38**, 1400; (b) N. Stock and S. Biswas, *Chem. Rev.*, 2012, **112**, 933; (c) R. Natarajan, G. Savitha, P. Dominiak, K. Wozniak and J. N. Moorthy, *Angew. Chem., Int. Ed.*, 2005, **44**, 2115.

7 (a) D. Wu, J. J. Gassensmith, D. Gouvêa, S. Ushakov, J. F. Stoddart, and A. Navrotsky, *J. Am. Chem. Soc.*, 2013, **135**, 6790; (b) R. Heck, J. Bacsa, J. E. Warren, M. J. Rosseinsky and D. Bradshaw, *CrystEngComm,* 2008, **10**, 1687; (c) X. L. Wang, C. Qin, S. X. Wu,

K. Z. Shao, Y. Q. Lan, S. Wang, D. X. Zhu, Z. M. Su and E. B. Wang, *Angew. Chem., Int. Ed.,* 2009, **48**, 5291; (d) F. Gross, E. Sherman, S. L. Mahoney, and J. J. Vajo, *J. Phys. Chem. A*., 2013, **117**, 3771.

8 (a) L. Ma and W. Lin, *J. Am. Chem. Soc.,* 2008, **130**, 13834; (b) X. Q. Lu, J. J. Jiang, C. L. Chen, B. S. Kang and C. Y. Su, *Inorg. Chem.,* 2005, **44**, 4515; (c) B. Zheng, H. Dong, J. Bai, Y. Li, S. Li and M. Scheer, *J. Am. Chem. Soc.,* 2008, **130**, 7778. (d) T. Ishiwata, Y. Furukawa, K. Sugikawa, K. Kokado, and K. Sada, *J. Am. Chem. Soc.*, 2013, **135**, 5427.

9 (a) N. Nijem, L. Z. Kong, Y. G. Zhao, H. H. Wu, J. Li, D. C. Langreth, and Y. J. Chabal, *J. Am. Chem. Soc.*, 2011, **133**, 4782; (b) B. Dey, S. R. Choudhury, P. Gamez, A. V. Vargiu, A. Robertazzi, C. Y. Chen, H. M. Lee, A. D. Jana and S. Mukhopadhyay, *J. Phys. Chem. A,* 2009, **113**, 8628; (c) A. Das, A. D. Jana, S. K. Seth, B. Dey, S. R. Choudhury, T. Kar, S. Mukhopadhyay, N. J. Singh, I. C. Hwang and K. S. Kim, *J. Phys. Chem. B,* 2010, **114**, 4166; (d) J. Canivet, S. Aguado, Y. Schuurman, and D. Farrusseng, *J. Am. Chem. Soc.*, 2013, **135**, 4195.

10 (a) X. Zhou, P. Liu, W. H. Huang, M. K., Y. Y. Wang and Q. Z. Shi, CrystEngComm, 2013, 15, 8125 (b) Z. W. Wang, C. C. Ji, J. Li, Z. J. Guo, Y. Z. Li and H. G. Zheng, Cryst. Growth Des., 2009, 9, 475. (c) Y. Q. Lan, H. L. Jiang, S.L. Li, and Q. Xu, Inorg. Chem., 2012, 51, 7484.

11 (a) W. Zhao, J. Han, G. Tian and X. L. Zhao, CrystEngComm, 2013, 15, 7522 (b) P. Kanoo, K. L. Gurunatha and T. K. Maji, Cryst. Growth Des., 2009, 9, 4147. (c) H. J. Li, B. Zhao, R. Ding, Y. Y. Jia, H. W. Hou, and Y. T. Fan, Cryst. Growth Des., 2012, 12, 4170.

12 (a) B. Mu, F. Li, K. S. Walton, Chem. Commun., 2009, 2493; (b) Z. L. Chen, C. F. Jiang, W. H. Yan, F. P. Liang and S. R. Batten, Inorg. Chem., 2009, **48**, 4674; (c) L. Chen, L. Zhang, S. L. Li, Y. Q. Qiu, K. Z. Shao, X. L. Wang and Z. M. Su, *CrystEngComm,* 2013, **15**, 8214.

13 (a) N. Chen, M. X. Li, P. Yang, X. He, M. Shao, and S. R. Zhu, *Cryst. Growth Des.*, 2013, **13**, 2650; (b) O. M. Yaghi, H. Li, C. Davis, D. Richardson and T. L. Groy, *Acc. Chem. Res.,* 1998, **31**, 474; (c) B. Chen, M. Eddaoudi, T. M. Reineke, J. W. Kampf, M. O'Keeffe and O. M. Yaghi, *J. Am. Chem. Soc.,* 2000, **122**, 11559; (d) J. Yang, J. F. Ma, Y. Y. Liu, J. C. Ma and S. R. Batten, *Cryst. Growth Des.,* 2009, **9**, 1894; (e) M. Sadakiyo, T. Yamada, and H. Kitagawa, *J. Am. Chem. Soc.*, 2011, **133**, 11050; (f) R. S. Forgan, R. A. Smaldone, J. J. Gassensmith, H. Furukawa, D. B. Cordes, Q. W. Li, C. E. Wilmer, Y. Y. Botros, R. Q. Snurr, A. M. Z. Slawin, and J. F. Stoddart, *J. Am. Chem. Soc.*, 2012, **134**, 406.

14 (a) J. L. C. Rowsell, E. C. Spencer, J. Eckert, J. A. K. Howard and O. M. Yaghi, *Science*, 2005, **309**, 1350; (b) H. Park, D. M. Moureau and J. B. Parise, *Chem. Mater.*, 2006, **18**, 525; (c) X. Y. Wang and S. C. Sevov, *Inorg. Chem.,* 2008, **47**, 1037; X. H. Lou, C. Xu, H. M. Li, Z. Q. Wang, H, Guo, and D. X. Xue, *CrystEngComm,* 2013, **15**, 4606.

15 (a) X. Feng,X. L. Ling, L. Liu, H. L. Song, L. Y. Wang, S. W. Ngd, and B. Y. Su, *Dalton Trans.,* 2013, **42**, 10292 (b) H. Park, D. M. Moureau and J. B. Parise, *Chem. Mater.,* 2006, **18**, 525. (c) J. Cepeda, R. Balda, G. Beobide, O. Castillo, J. Fernández, A. Luque, S. P. Yáñez, and P. Román *Inorg. Chem.,* 2012, **51**, 7875.

16 (a) D. Liu, Z. G. Xie, L. Q. Ma, and W. B. Lin, *Inorg. Chem.,* 2010, **49**, 9107; (c) H. Guo, G. Zhu, I. J. Hewitt and S. Qiu, *J. Am. Chem. Soc.,* 2009, **131**, 1646; (d) Y. Zou, M. Park, S. Hong and M. S. Lah, *Chem. Commun.,* 2008, 2340. (e) Y. X. Hu, H. B. Ma, B. Zheng, W. W. Zhang, S. C. Xiang, L. Zhai, L. F. Wang, B. L. Chen, X. M. Ren, and J. F. Bai, *Inorg. Chem.,* 2012, **51**, 7066.

17 (a) O. M. Yaghi, M. O'Keeffe, N. W. Ockwig, H. K. Chae, M. Eddaoudi and J. Kim, *Nature,* 2003, **423**, 705; (b) M. Eddaoudi, J. Rosi, N. Kim, D. Vodak, J. Wachter, M. O'Keefe and O. M. Yaghi, *Science,* 2002, **295**, 469; (c) H. Furukawa, J. Kim, N. W. Ockwig, M. O'Keeffe and O. M. Yaghi, *J. Am. Chem. Soc.,* 2008, **130**, 11650; (d) S. Vagin, A. Ott, H. C. Weiss, A. Karbach, D. Volkmer, and B. Rieger, *Eur. J. Inorg. Chem.* **2008, 2601** (e) N. L. Rosi, J. Eckert, M. Eddaoudi, D. T. Vodak, J. Kim, M. O 'Keeffe and O. M. Yaghi, *Science,* 2003, **300**, 1127.

18 (a) L. L. Zhang, F. L. Liu, Y. Guo, X. P. Wang, J. G., Y. H. Wei, Z. Chen, and D. F. Sun, *Cryst. Growth Des.,* 2012, **12**, 6215; (b) A. M. Fonseca, M. M. M. Raposo, A. M. R. C. Sousa, G. Kirsch, and M. Beley, *Eur. J. Inorg. Chem.,* 2005, **21**, 4361; (c) C. Pettinari, N. Masciocchi, L. Pandolfo and D. Pucci, *Chem.Eur. J.*, 2010, **16**, 1106; (d) H. Y. Zang, Y. Q. Lan, G. S. Yang, X. L. Wang, K. Z. Shao, G. J. Xu and Z. M. Su, *CrystEngComm,* 2010, **12**, 434; (e) S. Verma, A. K. Mishra and J. Kumar, Acc. Chem. Res., 2010, **43**, 79; (f) J. Rocha, F. A. A. Paz, F. N. Shi, R. A. S. Ferreira, T. Trindade, and L. D. Carlos, *Eur. J. Inorg. Chem.,* 2009, **33**, 4931.

19 F. F. Xing, J. Jia, L. C. Liu, L. N. Zhong, M. Shao, Y. L. Bai, Y. M. Zhao, S. R. Zhu, X. He, M. X. Li, *CrystEngComm*, 2013 ,**15**, 4970.

20 (a) L. Lisnard, L. M. Chamoreau, Y. L. Li, and Y. Journaux, *Cryst. Growth Des.,* 2012, **12**, 4955; (b) X. H. Chang, J. H. Qin, L. F. Ma, J. G. Wang, and L. Y. Wang, *Cryst. Growth Des.,* 2012, **12**, 4649; (c) J. S. Hu, L. F. Huang, X. Q. Yao, L. Qin, Y. Z. Li, Z. J. Guo, H. G. Zheng and Z. L. Xue, *Inorg. Chem..,* 2011, **50**, 2404; (d) S. K. Henninger, H. A. Habib and C. Janiak, *J. Am. Chem. Soc.,* 2009, **131**, 2776; (e) D. C. Zhong, J. H. Deng, X. Z. Luo, H. J. Liu, J. L. Zhong, K. J. Wang, and T. B. Lu *Cryst. Growth Des.*, 2012, **12**, 1992.

21 (a) J. Guo, D. Sun, L. L. Zhang, Q. Yang, X. L. Zhao, and D. F. Sun *Cryst. Growth Des.*, 2012, **12**, 5649; (b) H. A. Habib, A. Hoffmann, H. A. Ho¨ppe and C. Janiak, *Dalton Trans.*, 2009, 1742; (c) T. H. Park, K. Koh, A. G. W.Foy, and A. J. Matzger, *Crys. Growth Des.*, 2011, **11,** 2059; (d) Z. Shi, S, H. Feng, Y. Sun, and J. Hua, *Inorg. Chem.*, 2001, **40**, 5312; (e) Z. Su, J. Xu, J. Fan, D. J. Liu, Q. Chu, M. S. Chen, S. S. Chen, G. X. Liu, X. F. Wang and W. Y. Sun, Crys. Growth Des., 2009, **9**, 2801.

22 G. M. Sheldrick, SADABS: Empirical Absorption Correction Program, University of G€ ottingen: G€ ottingen, Germany, 1997.

23 XPREP, version 5.1. Siemens Industrial Automation Inc.: Madison, WI, 1995.

24 G. M. Sheldrick, SHELXS−97, Program for Crystal Structure Solution; Gottingen University: Germany, 1997.

25 (a) Y. J. Cui, Y. F. Yue, G. D. Qian, B. L. Chen, *Chem. Rev.,* 2012, **112**, 1126; (b) A. W. Adamson and P. D. Fleischauer, Concepts of Inorganic Photochemistry, John Wiley, New York, 1975.

26 (a) J. R. Lakowicz, Principles of Fluorescence Spectroscopy, 3rd edn, Springer, Berlin, 2006; (b) B. Valeur, Molecular Fluorescence: Principles and Application, Wiley VCH, Weinheim, 2002; (c) S. L. Zheng, J. H. Yang, X. L. Yu, X. M. Chen, W. T. Wong, *Inorg. Chem.,* 2004, **43**, 830.

27 (a) O. Kahn, Molecular Magnetism, Wiley−VCH, New York, 1993; (b) B. N. Figgis, Wiley Interscience, New York, 1961.

28 (a) J. C. Jeffery, P. Thornton, M. D. Ward, *Inorg. Chem.*, **1994**, 33, 3612. (b) H. R. Chang, S. K. Larsen, P. D. W. Boyd, C. G. Pierpont, D. N. Hendrickson, *J. Am. Chem. Soc.*, **1988**, 110, 4565; (c) M. Wesolek, D. Meyer, J. A. Osborn, A. Cian, J. Fischer, A. Derory, P. Legoll, M. Drillon, *Angew. Chem. Int. Ed. Engl.*, **1994**, 33, 1592.